Regio-Regular Oligo and Poly(3-hexyl thiophene): Precise Structural Markers from the Vibrational Spectra of Oligomer Single Crystals.

Luigi Brambilla,*[,†] Matteo Tommasini,[†] Ioan Botiz,[‡,§] Khosrow Rahimi,[∥] John O. Agumba,[⊥] Natalie Stingelin,[§] and Giuseppe Zerbi*[,†]

[†]Dipartimento di Chimica, Materiali e Ingegneria Chimica "G. Natta", Politecnico di Milano, Piazza Leonardo da Vinci 32, 20133 Milano Italy

[‡]Nanobiophotonics and Laser Microspectroscopy Center, Faculty of Physics and Interdisciplinary Research Institute in Bio-Nano-Sciences, Babes-Bolyai University, Treboniu Laurian Street 42, Cluj Napoca 400271, Romania

[§]Department of Materials, Imperial College London, Exhibition Road, London, SW7 2AZ, U.K.

[∥]DWI-Leibniz Institute for Interactive Materials, RWTH Aachen University, 52074 Aachen, Germany

[⊥]Institute of Physics, University of Freiburg, Hermann-Herder Strasse 3, Freiburg 79104, Germany

1. INTRODUCTION

Polythiophenes, and especially their alkyl derivatives, belong to the class of poly-conjugated materials, which are the center of strong interest of many academic and industrial laboratories and play a dominant role in the development of new technologies in the field of molecular electronics, optoelectronics, solar cells, and sensors.[1−6] The number of papers dealing with their characterization at the molecular and/or supra-molecular levels is large. However, while an overall knowledge of the molecular and crystalline structures of many of the materials of the family of poly(3-alkylthiophenes) can be considered satisfactorily acquired from experiments and calculations[7−12] more structural details are desirable for the understanding of the physical scenario which justifies the observed physical properties of interest to basic and applied sciences. Presently the unique role played by vibrational spectroscopy (Raman scattering in particular) in the structural studies of poly conjugated materials is unquestionable and made vibrational spectroscopy a commonly used tool for the study of the physics, chemistry and technology of this wide class of new materials.[13−16] The vibrational infrared spectra have been already extensively used (sometimes in conjunction with X-ray scattering DSC and ^{13}C NMR techniques) in the study of the crystal and molecular structures and of order/disorder phase transitions of regioregular poly(3-hexylthiophene) and poly(3-butylthiophene).[17−19]

The justification of the study reported in this paper is the fact that at present single crystals of a few regioregular oligo alkylthyiophenes and of regioregular poly alkyl-thiophene are available and their molecular and crystal structures have been carefully studied by selected areas electron diffraction (SAED).[20−22] We are reporting here for the first time their infrared and Raman spectra from which we extract new spectroscopic markers that can be correlated to specific molecular structures of ordered alkyl-thiophene units that, at the best of our knowledge, have never been reported before. These spectroscopic markers were not accessible up to now because they were hidden in the spectral pattern of the more disordered materials consisting of regioregular or regiorandom poly(3-hexylthiophene) extensively studied in previous works (e.g., refs 17−19).

Our study is supported by DFT quantum chemical calculations on "realistic" molecular models of the octamer of the (3-hexylthiophene) *with no chemical simplifications.* In our

Received: August 5, 2014
Revised: September 11, 2014
Published: October 3, 2014

study we have also employed theoretical and experimental results on the spectroscopic properties of the corresponding unsubstituted and parent molecules (i.e., oligo-thiophenes and *n*-alkanes) which have already been the subject of several investigations.[23−25]

What makes our work different from what discussed in the very abundant literature on the structural properties of alkyl substituted oligo and poly thiophenes is the fact that we take as reference the precise molecular structures of carefully prepared regioregular octa(3-hexylthiophene) single crystals.[20] In this work we present and discuss the experimental vibrational Infrared and Raman spectra of (i) single crystals (bundles of single crystal for the FT-IR experiments) and poly crystalline bulk material of regioregular octa(3-hexylthiophene) $(\mathbf{3HT})_8$, (ii) poly crystalline bulk material of regioregular trideca(3-hexylthiophene) $(\mathbf{3HT})_{13}$, and (iii) semicrystalline regioregular poly(3-hexylthiophene) (**P3HT**). We point our attention to new and specific vibrational features which can be assigned thanks to the fact that the chemistry and the structure of these materials are clean and well-studied in the literature.[20,26]

We wish to emphasize that in this work we have recorded and analyzed both the IR and Raman spectra which have provided complementary and converging information.

We propose a set of spectroscopic structural markers to be used by chemists and technologists for the molecular characterization of their P3HT-based materials and for the interpretation of their physical and chemical properties.

2. EXPERIMENTAL SECTION

Samples: octamer $(\mathbf{3HT})_8$ and tridecamer $(\mathbf{3HT})_{13}$ of 3-hexylthiophene were kindly provided by Felix P.V. Koch and Paul Smith and synthesized following the procedure described in ref 26; regioregular poly 3-hexyl-thiophene **P3HT** from Merck Chemicals, of weight-average molecular weight (M_n) of 26400 g/mol with a polydispersity index (PDI) of 1.79 and a regioregularity of 96.2% were used as received.

Single crystals of $(\mathbf{3HT})_8$ of M_n = 1332 g/mol, PDI = 1, and regioregularity of 100% were grown in tetrahydrofuran (THF) solution (10 mg/mL) at 2 °C for about 48 h after an initial dissolution at 25 °C[20,21] and deposited onto UV/ozone-cleaned SiO_2 wafers (Raman measurements) or NaCl windows (infrared measurements) using spin-casting method.

FT-Raman spectra of polycrystalline materials excited at 1064 nm were recorded with a Nicolet Nexus 9650 FT-Raman spectrometer equipped with 2W Nd:YAG laser, notch filter and XY microstage accessory. The spectra reported are the average of 1024 scan with a resolution of 4 cm^{-1} and a laser power at the sample of 200 mW. To prevent and/or reduce a possible laser-induced heating the samples were placed in close contact with the metallic sample holder of the XY-microstage.

Raman spectra of polycrystalline and single crystal $(\mathbf{3HT})_8$ excited at 785 nm were recorded with an Horiba Jobin Yvon Labram HR800-UV spectrometer coupled with an Olympus BX41 microscope using a 50X objective in a back scattering geometry. Spectra of samples deposited on silicon substrate were obtained as average of 4 spectra recorded with a laser power on the sample of a few milliwatts. For both Raman and FT-Raman experiment care was adopted to prevent laser-induced degradation of the sample and to ensure the reproducibility of the spectra.

Infrared Spectra have been collected with a Nicolet Nexus FT-IR spectrometer coupled with a Continμm infrared microscope and 15X Casgrain objectives. A bundle of single crystals of $(\mathbf{3HT})_8$ has been analyzed in transmission mode under the microscope on sample deposed on NaCl window. Polycrystalline samples of $(\mathbf{3HT})_8$, $(\mathbf{3HT})_{13}$ and **P3HT** have been recorded using a diamond anvil cell in order to obtain films of a few μm thickness. Temperature dependent spectra have been recorded with a Linkam FTIR-600 cell on samples deposited on ZnSe windows. For the experiments we considered 256 acquisitions with a resolution of 1 or 4 cm^{-1}. Experimental spectroscopic data on *n*-heneicosane ($C_{21}H_{44}$) and hexathiophene (**T6**) used in this paper have been taken from our database of spectra recorded in the laboratory. All the spectra reported in the figures have been normalized and are displayed offset to ease the comparison.

Calculations have been carried out by using the Gaussian09 computer code[27] on a small computer cluster operated by the group at the Department of Chemistry, Materials and Chemical Engineering (Politecnico di Milano). We have considered density functional theory (B3LYP/6-31G(d,p) level) as a viable method to deal with molecular models with realistic structure, while keeping under control the computational effort. For instance, the largest B3LYP/6-31G(d,p) model in this study $(\mathbf{3HT})_8$ consists of 202 atoms and has a basis set size of 1922, which is sizable for calculations of Raman spectra, requiring the Hessian and the derivatives of the polarizability. The method chosen is known to provide an appropriate description of vibrational spectra after adoption of suitable frequency scale factors.[28] In this work, we have considered the scale factor = 0.98, which has been empirically adopted in such a way to match the strongest Raman line and ease the comparison of the experimental and theoretical spectra.

3. MOLECULAR MODELS FROM DFT CALCULATIONS

As an overall general guideline in the discussion of the detailed molecular aspects of the molecules of interest we have considered DFT calculations (see Section 2) on realistic molecular models of $(\mathbf{3HT})_8$. For "realistic" in our calculations we mean that (i) we considered the full single molecule without any structural simplification and (ii) both free and constrained energy minimizations have been considered by starting, as input, from logical structures suggested by chemical common sense and from the data from SAED.

Given the relevant size of the molecular models, calculations have been carried out *in vacuo*, i.e., no simulation of intermolecular interactions have been attempted either by continuum solvation models or by calculations on dimers. The $(\mathbf{3HT})_8$ models obtained from calculations and the atom numbering adopted in this work are reported in Figure 1. The molecular structures can be described as follows:

(1) In structure A, the thiophene units in the backbone (hereafter denoted as the backbone) has been con-strained to be planar along the geometry optimization process, which started from a guess geometry extracted from the known crystal structure of $(\mathbf{3HT})_8$ that, from SAED measurements,[20] turns out to be similar to the so-called form II previously proposed for poly(3-alkylth-iophene).[7−9,29] To this aim, all dihedral angles (S−C2− C5′-S′) have been fixed at 180°. The hexyl chains were left free during the optimization. They assume the *all-trans*, conformation with the CCCC planes orthogonal to backbone plane. The dihedral angle $\tau(C_2C_3C_\alpha C_\beta)$ has a value of 90° and the chain axis is tilted by Θ = 140° with respect to the backbone axis.

(2) In structure B, to study a different extended planar geometry, we constrain the backbone to be planar, with extended *trans*planar hexyl chains which lie in the plane of the thiophene backbone; Θ = 90°, $\tau(C_2C_3C_\alpha C_\beta)$ = 180°.

(3) Structure C has been obtained by starting from the geometry of A. All planarity constraints on the backbone have been relaxed and a full geometry optimization has been carried out, leaving the system reaching its energetically more stable structure. Interestingly the

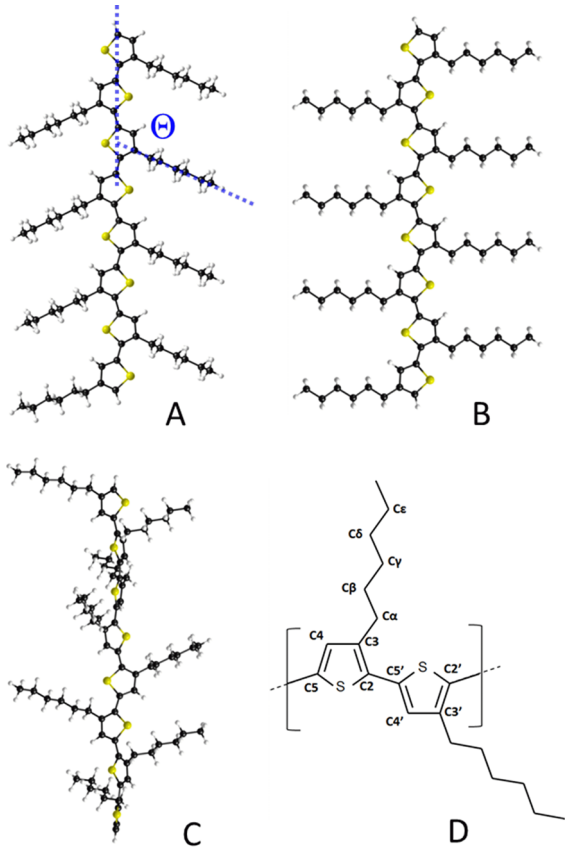

Figure 1. Molecular structures of regioregular $(\mathbf{3HT})_8$ obtained with DFT calculations: (A) molecular model with a geometry close to that of the molecule in the single crystal; (B) molecular model with coplanar thiophene rings and trans-planar alkyl chains; (C) fully optimized geometry. The chemical structure and atom numbering of the repeating unit of **P3HT** is also reported in panel D.

backbone takes an helix conformation (with $\tau(C_2C_3C_{5'}C_{4'}) = 35°$ for the central unit) while the hexyl chains remain *trans*-planar with the chain axis tilted by $\Theta = 40°$ and $\tau(C_2C_3C_\alpha C_\beta) = 90°$.

4. STRUCTURE AND PROPERTIES OF THE BACKBONE FROM RAMAN SPECTRA

Since the chain consists of a sequence of polyconjugated thiophene units, when using vibrational spectroscopy, especially Raman, we should consider the physical phenomena associated with the delocalization of π electrons along the backbone. The related phenomena observed have been matter of many papers, just after polyacetylene $-(HC{=}CH)-$ had made its appearance.[30−36] The communities of chemistry and physics developed two formally independent lines of thought in the interpretation of the observed properties of polyacetylene and of the many other polyconjugated materials (including also polythiophenes) synthesized by a crowd of chemists. For many years the two communities described the observed phenomena with untranslatable languages. In this paper, we adopt the physicochemical language for a constructive approach to the chemical community. In the early stages of the science of polyacetylene the interpretation of its Raman spectrum formed the basis for the description of the peculiar molecular dynamics and spectroscopy of polyconjugated materials. The interested reader may consult the abundant literature on these matters.[32−36]

The basic concept is that when a molecular chain with adjacent sp^2 carbon atoms allows the delocalization of π electrons along its backbone, the longer the chain is the lower the HOMO−LUMO energy gap becomes;[37] it follows that the color darkens and the system may become an electrical conductor if suitably doped. For many polyconjugated materials photoconductivity[38] and unusual nonlinear optical properties[39,40] may be attained. These properties have caused the interest of Physics and Chemistry and have attracted great attention by modern technology and industry.[41]

The Raman spectra of polyconjugated materials show characteristic features, namely a very strong line is observed over the energy range of the C═C stretching modes (1600−1400 cm^{-1}) and it was first signaled as unusual Raman feature by Rimai[42] who was working on carotenoids. This mode cannot be simply assigned to the traditional "group frequency"[43,44] C═C stretching mode, but has to be considered as the result of a collective skeletal stretching (traditionally indicated with the cyrillic letter Я) of the whole polyconjugated chain or of a relatively long portion of it. The frequency of this mode is strongly affected by the collective delocalization of π electrons along such one-dimensional lattice as the result of a strong electron−phonon coupling.[32−36]

Theory predicts that the frequency of the Я mode shows dispersion with the effective conjugation length (ECL), which is not a physical chain length, and shows a superlinear dispersion of the intensity when the excitation energy approaches the HOMO−LUMO gap (resonance Raman condition), associated with a given chain length characterized by its own ECL.[32] The extent of delocalization strongly depends on the system considered and on its geometry which modulates the overlapping of adjacent $2p_z$ orbitals. Other lines of relatively less importance can be observed depending on the chemical and structural nature of the material. Of particular relevance for the present work is the fact that the *Raman activity of the other normal modes depends mostly on the extent of coupling with the Я mode,* as discussed in details in refs 13, 14, and 32.

4.1. Raman spectra of crystalline and polycrystalline $(\mathbf{3HT})_8$. In Figure 2a we compare the experimental Raman spectra of bulk polycrystalline and single crystal $(\mathbf{3HT})_8$ samples. The marked difference between the two spectra is due to the fact that the scattering of the Я mode near 1448 cm^{-1} and of a few other lines for the single crystal appears strongly reduced with respect to other Raman lines at lower wavenumbers. As shown in Figure 2a when considering the single crystal structure of $(\mathbf{3HT})_8$ as determined by SAED,[20,21] the thiophene backbones are perpendicular to the crystal top face and are parallel to the direction of the laser beam (z axis). It follows that in the scattering geometry adopted in Figure 2a the normal modes (such as the Я modes) whose main element (zz) of the polarizability tensor derivative is along the π-conjugated backbone do show reduced Raman intensity.

For this reason, we have to base our Raman analysis on polycrystalline $(\mathbf{3HT})_8$ samples where microcrystals with all possible orientations are expected (as confirmed by IR) so that all Raman lines can be reliably observed.

In Figure 2b, we report the calculated Raman spectra of the models of $(\mathbf{3HT})_8$ compared with the experimental Raman spectrum of polycrystalline $(\mathbf{3HT})_8$. The first observation is that the results of quantum chemical calculations undoubtedly favor structure A as the one more representative of the

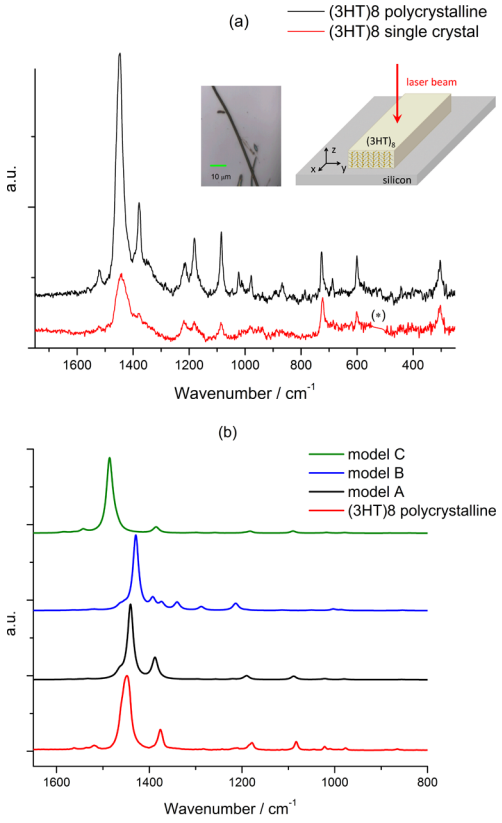

Figure 2. (a) Experimental Raman spectra excited at 785 nm of $(\mathbf{3HT})_8$: single crystal (red line) and polycrystalline (black line). The single crystal analyzed is shown in the inset. (*)Si line at 520 cm^{-1} has been removed for clarity. (b) Comparison among the experimental Raman spectrum of polycrystalline $(\mathbf{3HT})_8$ excited at 1064 nm (red line) and the DFT calculated Raman spectra, scaled by a factor of 0.98, of models of Figure 1: A (black line), B (blue line), and C (green line).

experimental Raman features. Model B shows a larger number of Raman lines in the 1400−1100 cm^{-1} range and model C shows an upshift of the Я mode peak, obviously associated with the decrease of π-conjugation caused by the torsion about the interthiophene C−C bonds.[13,14,32]

In Figure 3 the Raman spectra in the range 1600−200 cm^{-1} of solid and $CHCl_3$ solution of $(\mathbf{3HT})_8$ are compared with the

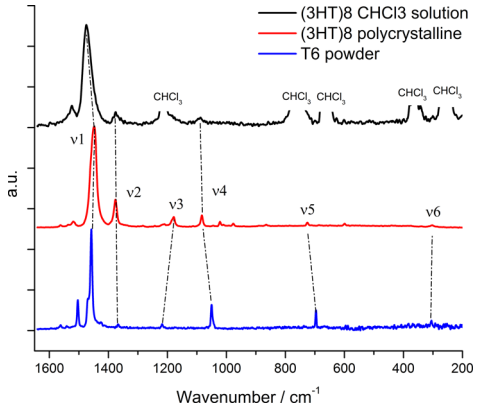

Figure 3. Raman spectra excited at 1064 nm of: solid hexathiophene (**T6**) (blue line), polycrystalline $(\mathbf{3HT})_8$ (red line), and $(\mathbf{3HT})_8$ in chloroform solution (black line). Chloroform bands have been removed for clarity.

spectrum of hexathiophene (**T6**) taken as reference molecular model. In the spectral pattern of $(\mathbf{3HT})_8$ we find the six expected totally symmetric Raman lines associated with the vibrations of the thiophene backbone in the 1500−200 cm^{-1} range.[23]

The strong line at 1448 cm^{-1} (ν_1) can be immediately related to the "totally symmetric" Я mode clearly exhibited, as might be expected, in the spectrum of oligo and/or polythiophene chains in a "coplanar" structure.[23] When the backbone becomes conformationally distorted at C2−C5′ we expect that ν_1 shifts toward higher wavenumbers because of the decrease of ECL. This is indeed observed at 1475 cm^{-1}in the Raman spectra of $(\mathbf{3HT})_8$ in chloroform solution (see Figure 3) where it can be expected that the backbone is conformationally distorted. In Figure 3 we observe that the profile of ν_1 in the solid phase is asymmetric on the high frequencies side while in solution phase it is asymmetric on the low frequencies side. This asymmetry may be due to the $>CH_2$ and $-CH_3$ scissoring group modes of the hexyl chains occurring just in the same frequency range (near 1450 cm^{-1} both in solid and in solution) and may contribute, even if weakly, to Raman scattering.

Some additional observations on the Raman spectra and vibrational dynamics of these systems are worth to be pointed out and may deserve further studies. A medium-strong line at 1376 cm^{-1} (hereafter referred as ν_2) is observed in the spectrum of $(\mathbf{3HT})_8$ and appears as a negligibly weak line in the spectrum of **T6** (see Figure 3) and should not be confused with the umbrella motion of the $-CH_3$ group located at the end of the alkyl chains (which is clearly observed in the IR, near 1375 cm^{-1}). Such almost accidental degeneracy may be misleading when the vibrational spectra are interpreted simply and traditionally based on "group frequencies".[40,41]

The calculated vibrational displacements show that ν_2 originates from the dynamical coupling of the vibrations of the backbone with those of the alkyl substituents and can be described as the coupling of the stretching of C_3-C_4 and $C_3{=}C_2$ while $C_2-C_{5'}$ and $C_{5'}{=}C_{4'}$ do not move. It is clear that ν_2 is not a collective mode and should not show frequency and intensity dispersion with excitation energy or with the changing in the ECL; in fact its frequency does not change from solid to solution, opposite to ν_1. However, the position and intensity of ν_2 could be modulated either by chemical substitution in C_3 and $C_{3'}$ or by structural disorder. For instance, the relative intensity of ν_2 in **T6** is significantly lower compared to $(\mathbf{3HT})_8$ (see Figure 3).

In the 1300−200 cm^{-1} range additional Raman lines much weaker than the Я mode are observed for $(\mathbf{3HT})_8$ (Figure 3). They do not occur in the spectra of **T6** (see Figure 3) and can be ascribed to normal modes resulting from the coupling of the vibrations of the backbone with those of the alkyl substituents.[13,14] Normal mode analysis from DFT calculations clarifies that the vibrations giving rise to the scattering centered at 1000 cm^{-1} are mostly localized in the stretching of the C_3-C_α (and $C_{4'}-C_{\alpha'}$) bond coupled with the skeletal deformation of the thiophene ring to which it is attached.

4.2. Structural Markers from the Raman Spectra of Polycrystalline $(\mathbf{3HT})_8$ and $(\mathbf{3HT})_{13}$ and Solid P3HT. Very relevant in the understanding of the structural properties of these systems is the comparison of the three experimental Raman spectra of polycrystalline $(\mathbf{3HT})_8$, $(\mathbf{3HT})_{13}$ and solid **P3HT** reported in Figure 4, parts a and b. The spectra of $(\mathbf{3HT})_8$ and $(\mathbf{3HT})_{13}$ are practically identical both in the 1400 cm^{-1} range, as well as in the sequence of signals extending from

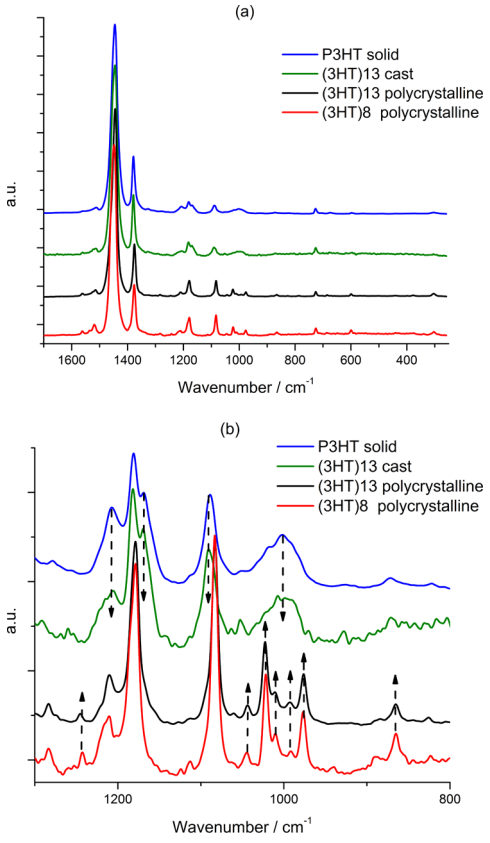

Figure 4. (a) Survey of the Raman spectra excited at 1064 nm of polycrystalline $(\mathbf{3HT})_8$ (red line), polycrystalline $(\mathbf{3HT})_{13}$ (black line), cast $(\mathbf{3HT})_{13}$ (green line), and solid **P3HT** (blue line). (b) Details of the Raman spectra in the 700−1300 cm^{-1} region showing signals due to alkyl chain order for $(\mathbf{3HT})_8$, $(\mathbf{3HT})_{13}$ (up arrows) and disorder for cast $(\mathbf{3HT})_{13}$ and solid **P3HT** (down arrows).

1400 to 700 cm^{-1}. On the contrary, the Raman spectrum of **P3HT** shows additional lines in the same range. Moreover, the weak lines are noticeably broader, particularly the line near 1000 cm^{-1} which turns out to be a convolution of several transitions necessarily associated with the fact that the hexyl side chains are conformationally distorted, thus indicating that the material contains structurally new species.

The existence of disorder on the side chains does not imply that the thiophene backbone be nonplanar as witnessed by the fact that the frequency of the strong ν_1 mode keeps the same value near 1445 cm^{-1} for all solid samples. The conformational distortion of the backbone becomes unquestionable upon suitable thermal treatment or in solution, where the ν_1 line is blue-shifted to 1475 cm^{-1} as a result of a decrease of π delocalization because of a torsion about the inter-ring C−C bond (see Figure 3). This observation suggests that in the solid state these materials may exists in two phases where phase 2 consists practically of a coplanar backbone surrounded by all-*trans* hexyl chains with $\tau(C_2C_3C_\alpha C_\beta) = 90°$ (e.g., model A) and phase 1 where the backbone is still flat while the hexyl chains (like hairs) are conformationally disordered with a distribution of torsional angles. It is worth noticing that the markers of disorder recorded for the **P3HT** are exactly the same as those observed in the Raman spectrum of $(\mathbf{3HT})_{13}$ cast from $CHCl_3$ solution where the backbone becomes flat, but the hexyl chains remain disordered (see Figure 4).

It can be concluded that simply from the Raman lines (1200−700 cm^{-1}) of the material in the solid state it becomes possible to distinguish whether the system has to be considered as totally ordered, with both backbone and hexyl chains all in a well-established conformation (phase 2) or whether, the backbone remains flat while the hexyl residues are distorted in a sort of hairy conformation (phase 1).

5. STRUCTURAL MARKERS FROM INFRARED

Figure 5 reports the IR spectra recorded in transmission mode of $(\mathbf{3HT})_8$ as: (i) a bundle of single crystals (shown in the inset

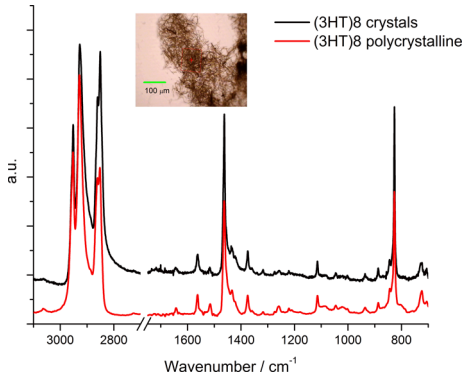

Figure 5. IR spectra of $(\mathbf{3HT})_8$: polycrystalline sample in a diamond anvil cell (red line) and bundle of single crystals deposited on NaCl window (black line). The bundle of crystals analyzed is shown in the inset.

of Figure 5) and (ii) in the polycrystalline state. The two spectral patterns appear very similar showing the same features that will be discussed below. Normally, from the IR spectra nothing can be said on the structure of the crystalline lattice.[45,46] However, by comparing the spectra of the polycrystalline and single crystals we can state that the structures of the molecules in the two samples are the same.

5.1. Thiophene (sp^2) CH Stretching Mode. Information on the properties of the backbone also come from the stretching frequency of the *only* CH bonds (with sp^2 C) in positions 4 and 4′ observed in the infrared near 3000 cm^{-1} as relatively very weak and broad band (see Figure 6). This weak IR signal has been fully rationalized, in general, in terms of CH bond length and atomic charges.[47] We consider these bands as arising from "local modes"[48] (we neglect to consider the

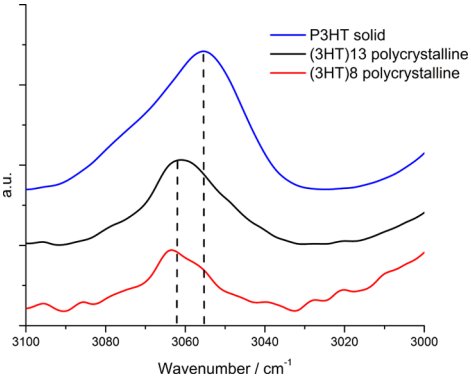

Figure 6. (sp^2) C_4−H stretching absorption of thiophene ring: polycrystalline $(\mathbf{3HT})_8$ (red line), polycrystalline $(\mathbf{3HT})_{13}$ (black line), and solid **P3HT** (blue line).

possible existence of overtones and combinations in Fermi resonance which may appear as very weak wiggles in the background). Following the approach proposed by McKean[49] we can then derive from the observed frequencies the bond length of the CH bond and the approximate atomic charge of the H atoms.[47]

It has been already shown that CH stretching frequencies in the pentagonal heteroaromatics change with the heteroatom.[50] If we focus on the data for the thiophene monomer the stretching of the CH bond in position 4 is observed at 3093 cm^{-1} in the vapor phase, at 3081 cm^{-1} in the liquid phase[51] and near 3080 cm^{-1} in the solid phase (measured in our laboratory). In Figure 6 the same absorption for crystalline $(3HT)_8$ and $(3HT)_{13}$ appears at 3061 and 3063 cm^{-1} respectively and at 3055 cm^{-1} both for a cast film of $(3HT)_{13}$ and for solid **P3HT**. The frequency downshift from crystalline phase to cast film (and, overall, with respect to thiophene) is unquestionable. Following McKean,[49] we can conclude that upon changing the molecular environment, the electronic structure of the σ bonds in the sp^2 CH is modified. The bond length increases, the force constant of the C−H bond weakens and the atomic charges on the hydrogen atoms increase. These changes are not to be taken as insignificant since we are dealing with carbon and hydrogen linked by rather strong σ bonds. The physics behind such changes is still worth investigating. So far we can envisage the existence of a phase-dependent mean field, which can affect the electronic structure of the CH bonds.

5.2. Hexyl Chains (sp^3) $>CH_2$ and $-CH_3$ Stretching and Bending Modes. Next we focus our attention on the vibrations of the alkyl chains for poly crystalline $(3HT)_8$ and $(3HT)_{13}$ and solid **P3HT**. The information derived is complementary to provide a deeper understanding of the structure of the *n*-alkanes, in general, and in particular of the materials under study. We discuss in a parallel way the $>CH_2$ and $-CH_3$ stretching and bending/wagging vibrations. The vibrational assignment in these regions is discussed below following the classical "group frequency" correlations.[43,44]

In Figure 7 we report the spectra of the samples in the 3000−2800 cm^{-1} range. The absorptions in this region are routinely assigned to the CH stretching of the $-CH_3$ and $>CH_2$ groups of the alkyl chains that in our sample are grafted in positions 3 of the thiophene units forming a regioregular system.

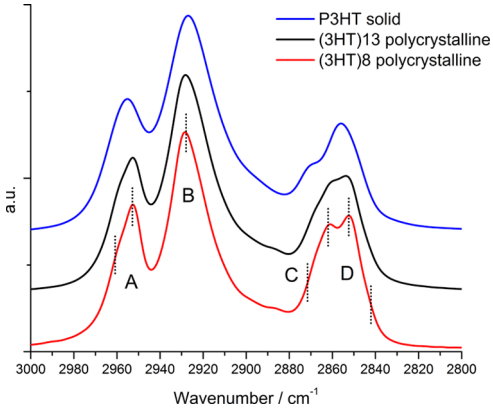

Figure 7. (sp^3) $>CH_2$ and $-CH_3$ stretching absorption of the hexyl chains for: polycrystalline $(3HT)_8$ (red line), polycrystalline $(3HT)_{13}$ (black line), and solid **P3HT** (blue line).

Band A is a doublet (2960, 2952 cm^{-1}) observed for $(3HT)_8$ and $(3HT)_{13}$ but not for **P3HT**, which shows a single component. As traditional, it is assigned, roughly speaking, to the "doubly degenerate" antisymmetric $-CH_3$ stretching. This mode is doubly degenerate when a 3-fold symmetry axis exists; when symmetry lowers it splits into two components. When the environment around the $-CH_3$ becomes fully disordered the doublet coalesces in a broad single band.

Band B (2929 cm^{-1}) is assigned to the antisymmetric $>CH_2$ stretching.

Band C (broad shoulder near 2870 cm^{-1}) is assigned to the symmetric $-CH_3$ stretching.

Band D is structured (2861, 2851, 2843 cm^{-1}) for $(3HT)_8$ and $(3HT)_{13}$ but it is single (2856 cm^{-1}) for **P3HT**. This is assigned, on the whole, to the symmetric $>CH_2$ stretching (see below).

For the class of *n*-alkanes Snyder and Schachtschneider[51] have very successfully shown that, when chains are *trans*-planar, the dynamics of 1-d crystals can be applied and we learn that $>CH_2$ stretching, $>CH_2$ bending, $>CH_2$ wagging, $>CH_2$ twisting and $>CH_2$ rocking motions generate sequences of IR active transitions (which are associated to $\mathbf{q} \neq 0$ phonons with $|\mathbf{q}| = \varphi/d$ and d the repeat distance; φ is the phase coupling between translationally equivalent oscillators). For shorter *trans*-planar chains, as the hexyl residues of **P3HT**, the vibrations of the $>CH_2$ groups are coupled with the vibrations of the end groups; notable vibrations of the end group are the $-CH_3$ umbrella motion ($\nu_U^{-CH_3}$ = 1375 cm^{-1}) and the external rocking motion ($\nu_{rock}^{-CH_3}$ = 890 cm^{-1}) for the end with the conformation $-CH_2^T-CH_2^T-CH_2-CH_3$. The concept of phase shift may not be any more rigorously valid and a few of the modes expected in this frequency range may give rise to selectively isolated and narrow lines. If the hexyl residues lose their conformational order, the fine structure disappears and broad bands may be observed. Thus, *we consider the observation of a fine structure in the band D as an indication of extended order, i.e., of the existence of hexyl residues in trans conformation with an intrachain order,* as it occurs indeed in $(3HT)_8$ single crystal and poly crystalline $(3HT)_8$ and $(3HT)_{13}$. On the other hand, the unstructured $>CH_2$ symmetric stretching indicates an *intra*-chain conformational disorder in the hexyl residue, just like in the case of solid **P3HT** or in the molten state of $(3HT)_8$ and $(3HT)_{13}$.

Information on the conformations of the hexyl chains come also from $>CH_2$ bending and (partly) wagging motions in the 1500−1300 cm^{-1} range reported in Figure 8. The IR spectra of $(3HT)_8$, $(3HT)_{13}$ and **P3HT** show differences which can be interpreted on the basis of the previous studies on the spectroscopy of the conformational defects in *n*-alkanes started by the school of Snyder[53] and later developed by the group in Milano.[54] These studies focused at the perturbations induced in the IR and Raman spectra of all *trans* chains by structural defects such as conformations or chain ends. These works have established that when *n*-alkane chains are conformationally distorted the vibrations of $>CH_2$ bending/wagging give rise to specific defect modes[53,54] mostly localized at the defect sites and give rise to absorption bands which can be taken as specific markers of the defects (e.g., G and GG at 1352 cm^{-1}, GTG and GTG′ at 1369 and 1306 cm^{-1}, etc.). Generally for *trans* alkyl chains the intensities of $>CH_2$ waggings are very weak, but those involved in the defect gain intensity because the electronic charge flux along the *trans* C−C chain is interrupted at the defect.[55]

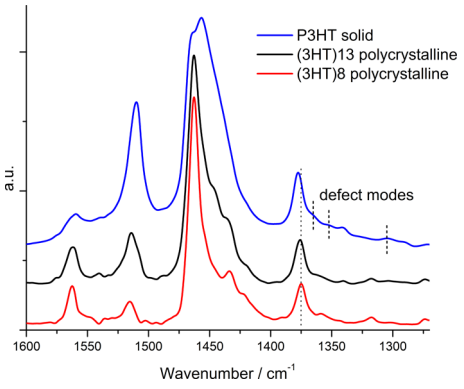

Figure 8. IR spectra in the region 1200−1600 cm^{-1} of polycrystalline $(\mathbf{3HT})_8$ (red line), polycrystalline $(\mathbf{3HT})_{13}$ (black line), and solid **P3HT** (blue line). The absorption due to the defect modes of conformationally distorted hexyl chains are indicated.

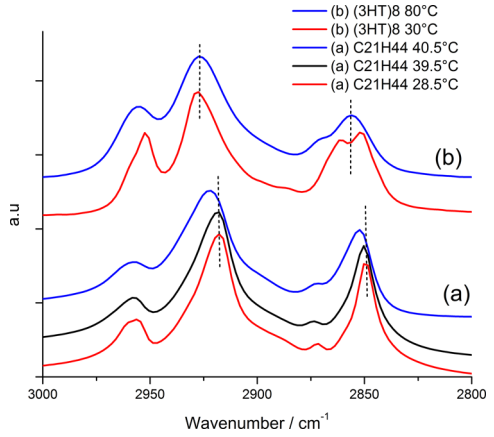

Figure 9. IR spectra in the $>CH_2$ and $-CH_3$ stretching region. Group (a): $C_{21}H_{44}$ crystalline at 28.5 °C (red line), α phase at 39.5 °C (black line), and melt at 40.5 °C (blue line). Group (b): $(\mathbf{3HT})_8$ polycrystalline at 30 °C (red line) and melt at 80 °C (blue line).

Let us take the $C_{21}H_{44}$ as a prototype case that can be compared with the spectra of the systems under study. $C_{21}H_{44}$ crystallizes in the orthorhombic lattice with two all-*trans* chains in the unit cell. In the $>CH_2$ bending region we expect that the **q**=0 bending mode splits into a doublet (observed at 1465 and 1473 cm^{-1}) because of factor group splitting for a molecule in an orthorhombic lattice caused by *the rather strong intermolecular potential* acting between *trans*-planar chains. Just before melting (T = 32.7 °C) the system undergoes a phase transition, to the so-called "α phase", where the *inter*chain potential is turned off and the doublet coalesces in a single band (1468 cm^{-1}) with *practically no indication of defect modes in the 1375−1300 cm^{-1} range.* At T = 40 °C the system melts with the appearance of characteristic defect modes observed at 1369, 1352, and 1306 cm^{-1} on the lower frequency side of $\nu_U{}^{-CH_3}$ = 1375 cm^{-1}.

Let us now consider the compounds under study (Figure 8): in the case of polycrystalline $(\mathbf{3HT})_8$ the $>CH_2$ bending band at 1462 cm^{-1} is strong and sharp. No broadening is observed in the range of 1450−1400 cm^{-1} as well as no defect modes appear on the lower frequency wavenumbers wing of $\nu_U{}^{CH_3-CH_3}$=1375 cm^{-1}. We conclude that in polycrystalline $(\mathbf{3HT})_8$ the hexyl chains are all, on the average, *trans*-planar. Polycrystalline $(\mathbf{3HT})_{13}$ shows a somewhat broader $>CH_2$ bending with $\nu_U{}^{-CH_3}$ = 1376 cm^{-1}, but practically no defect modes appear. Thus, in polycrystalline $(\mathbf{3HT})_{13}$ most of the chains are *trans*-planar and just a relatively small concentration of defects occurs. On the contrary, solid **P3HT** shows a broad $>CH_2$ bending ($\nu_U{}^{-CH_3}$ = 1378 cm^{-1}) and a fine structure of the defect modes on the lower frequency wing of $\nu_U{}^{-CH_3}$. This indicates that a fraction of hexyl chains are conformationally distorted, as expected for a semicrystalline material.

Once the structure of the *n*-alkyl residues has been established from the IR spectra we can derive a qualitative description of the interchain potential present in the various phases, i.e., crystal phase, α-phase (or rotatory phase), molten state.[69] In Figure 9, we report the comparison of the CH stretching signals observed for the hexyl residues in $(\mathbf{3HT})_8$ vs those observed in $C_{21}H_{44}$ (taken as prototypical alkane molecule). This comparison provides further information on the dynamics of the alkyl chains. At room temperature $C_{21}H_{44}$ shows the B band at $\nu_B{}^{C_{21}H_{44}}{}_{cryst}$ = 2917 cm^{-1}; in the "α-phase", or "rotatory phase", (39.5 °C) this band shifts to $\nu_B{}^{C_{21}H_{44}}{}_{\alpha}$ = 2918 cm^{-1} and just after melting (43.3 °C) it shifts to $\nu_B{}^{C_{21}H_{44}}{}_{melt}$ = 2923 cm^{-1} (Figure 9a). For polycrystalline $(\mathbf{3HT})_8$ (where the conformational markers of $>CH_2$ bending indicate fully *trans* hexyl chains) band B is observed at $\nu_B{}^{(3HT)_8}{}_{cryst}$ = 2928 cm^{-1} and keeps the same frequency upon melting, where the hexyl chains are conformationally disordered. In summary, three observations are to be accounted for:

(i) $\nu_B{}^{C_{21}H_{44}}{}_{cryst}$ (all-*trans* chains) < $\nu_B{}^{(3HT)_8}{}_{cryst}$ (all-*trans* hexyl chains)
(ii) $\nu_B{}^{C_{21}H_{44}}{}_{melt} \approx \nu_B{}^{(3HT)_8}{}_{cryst}$
(iii) $\Delta\nu_B$ (crystalline-melt) for $C_{21}H_{44}$ = 6 cm^{-1} while for $(\mathbf{3HT})_8$ = 0 cm^{-1}.

Necessarily, these differences must be ascribed to the strength of the *inter*alkyl chain potential which certainly differs for crystalline orthorhombic *n*-alkanes and for crystalline $(\mathbf{3HT})_8$. The change of the strength of the *inter*chain potential in the case of *n*-alkanes is "measured" by the values of $\Delta\nu_B{}^{C_{21}H_{44}}$ = 6 cm^{-1} and $\Delta\nu_B{}^{(3HT)_8}$ = 0. From these data it can be inferred that in crystalline $(\mathbf{3HT})_8$ the all-*trans* hexyl chains feel an intermolecular mean field certainly much weaker than that conceivable for the orthorhombic lattice of $C_{21}H_{24}$. It follows that for the hexyl residues in $(\mathbf{3HT})_8$ the torsional potential energy around the all-*trans* equilibrium is flatter, the vibrational displacements due to torsional motions may be relatively large and the dynamics of the chain may allow for a greater roto-torsional flexibility.

The propagation of conformational kinks along the *n*-alkane chains in a crystal has been at the center of interest for several years. A computational modeling by Klein[63] developed the idea of the generation, existence and propagation of "kinks" or of some sort of conformational solitons[65] with a consequent transport of matter which was experimentally observed by IR[66] and by STM[67] and justified theoretically.[68] All these works support the idea that an interlamellar molecular diffusion can occur, which is driven by suitable gearing of conformational distortions of the alkane chains in the solid state. In the molecules of this work the alkyl chains are definitely short and are bound to the thiophene backbone; however in a weak *inter*molecular potential they may experience large amplitude (temperature dependent) torsional motions. This scenario offers the justification of the idea that the hexyl chains may be involved in an *inter*-chain gearing (necessarily limited to a few CH_2 groups) which plays a role in the process of temperature-dependent interlocking of the hexyl chains during the phase

transformations amorphous → hairy rod → crystal and vice versa.

5.3. =C−H Out-of-Plane Deformation Modes: From Lamellar to Hairy Structures. Enough body of theoretical and experimental evidence associates the out-of-plane =C−H motion to an IR active transition (with large dipole strength) near 800 cm^{-1}. This transition shows to depend on the phase of the material and is somehow related to the geometry of the backbone and possibly to its electronic structure.

In Figure 10, the $(3HT)_8$ single crystals (as well as the polycrystalline) and the polycrystalline $(3HT)_{13}$ show a very

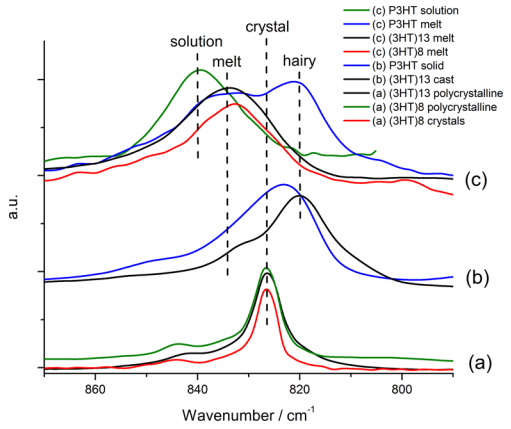

Figure 10. IR spectra in the region of the =CH out-of-plane vibration. Group (a): $(3HT)_8$ single crystal (red line), polycrystalline $(3HT)_8$ (green line) and polycrystalline $(3HT)_{13}$ (black line). Group (b): $(3HT)_{13}$ cast film from $CHCl_3$ solution (black line) and solid **P3HT** (blue line). Group (c): melt $(3HT)_8$ (red line), melt $(3HT)_{13}$ (black line), **P3HT** at 240 °C (blue line) and **P3HT** in $CHCl_3$ solution (green line).

sharp, narrow, symmetric, and strong line at 826 cm^{-1}. Necessarily, this band must be associated with the out-of-plane deformation of the =CH group of the structurally "ordered" molecule which, in agreement with the other IR/Raman spectral markers and SAED data,[20] can be described as structures with fully planar thiophene backbone, with iso-oriented and interlocked all-*trans* hexyl chains. *This band at 826 cm^{-1} can be thought to originate from the material in a crystal phase which is commonly labeled as form II.*[9,11,27]

On the other hand, for $(3HT)_{13}$ cast film from $CHCl_3$ solution onto a NaCl substrate, (with no annealing process applied), as well as for solid **P3HT**, the =CH out-of-plane band broadens noticeably and appears at 820 cm^{-1}. The breath is due to the convolution of vibrational transitions arising from sections of the backbone (still flat, see below) where the alkyl chains are grafted to the thiophene ring in β' with a distribution of $\tau(C_2C_3C_\alpha C_\beta)$ angles *in a disordered and possibly distorted geometry (hairy), thus perturbing the dynamics of the whole system.* We notice that in this hairy phase the thiophene backbone is lying flat, since the Raman ν_1 mode is unchanged compared to the polycrystalline phase (see Figure 4).

When both $(3HT)_8$ and $(3HT)_{13}$ are heated and brought to the melt state (80 and 170 °C, respectively) the =CH out-of-plane band broadens noticeably and it is peaked at 833 cm^{-1}. For the **P3HT** at the highest temperature achievable (240 °C) a large fraction of the backbone of **P3HT** is still flat since the feature assigned to the hairy phase (820 cm^{-1}) is observed (see Figure 10). The other spectral markers observed (>CH_2 and −CH_3 stretching and bending) indicate with certainty that the conformation of the hexyl chains has collapsed, thus producing a disordered phase (melt or amorphous state). If the force constant of the =C−H out of plane motion ($F_{\gamma opla}$) depends on the "twisting" angle of the backbone and increases with the increase of the twisting, the whole result is that we are seeing the spectrum of twisted backbone chains surrounded by hairs with collapsed disordered conformations. *The observed broad band at 833 cm^{-1} is to be considered as the convolution of the =CH out-of-plane signals of all these disordered structures (disordered/amorphous phase).* This is confirmed by the spectrum of **P3HT** in $CHCl_3$ solution (see Figure 10), where the backbone is certainly not planar, which shows a broad absorption band centered at 840 cm^{-1}. According to the discussion above, we may state the following:

(i) the broad band at 820 cm^{-1} is characteristic of the material in phase 1 (hairy);
(ii) the sharp band at 826 cm^{-1} is characteristic of the material in phase 2 (form II crystalline state);
(iii) the broad band at 833 cm^{-1} indicates the distorted/amorphous phase.

6. MOLECULAR STRUCTURE OF P3HT

On the basis of the above results and discussion, we propose here a description of the structure of the commercial **P3HT** used in this work. A fraction of the sample is clearly in phase 2, and it is embedded in a distribution of domains with distorted backbone and conformationally disordered hexyl chains. The relative populations of these structures depend upon the molecular weight and the thermal treatment of the sample. The "fringed micelle model" is a reasonable description of the structure. The quantification of the relative populations of the molecular structures identified by our spectroscopic observations is beyond the purpose of this paper, which first focuses on the detailed assignment of the vibrational spectra of **P3HT** related systems.

7. CONCLUSIONS

A conclusion of general relevance is that regioregular oligo and poly(3-hexyl-thiophene) may exist in three different phases that can be clearly distinguished with the help of IR and Raman spectroscopic markers. In the solid we identify: (i) **phase 1** or *hairy phase*, where the thiophene units of the backbone are coplanar with the grafted hexyl chains randomly oriented in space and with random conformations and (ii) **phase 2**, perfect *single crystal*, for the oligomers, where the backbones are planar and the trans-planar hexyl chains possess the same orientation. In the melt and in solution we identify **phase 3**, *distorted/amorphous*, where the thiophene backbones as well as the alkyl side chains are conformationally distorted.

The spectroscopic markers are the following:

(1) The frequency of the strong ***R*** *Raman mode* (ν_1) is the unambiguous marker of the shape of the thiophene backbone: *planar backbone* ν_1 = 1445 cm^{-1}, *distorted backbone* ν_1 = 1475 cm^{-1}.
(2) The medium-weak Raman pattern centered at 1000 cm^{-1} is the marker of the conformation of the hexyl chains grafted on the thiophene backbone. Conformationally ordered alkyl chains, as in the lamella, give rise to well-defined pattern of medium intensity sharp lines. Conformationally disordered alkyl chains with random

orientation, can be distinguished by a broad and structured scattering.

(3) The existence of intramolecular conformational order or disorder in the alkyl chains is indicated by the shape and width of the IR absorption in the 1500−1300 cm^{-1} range. All-trans chains give rise to a sharp infrared peaks at 1462 cm^{-1} (>CH_2 bending) and at 1375 cm^{-1} (−CH_3 umbrella motion). For conformational disordered chains an asymmetric structured large wing extending from 1480 to 1400 cm^{-1} appears and the −CH_3 umbrella band shifts slightly upward by a few wavenumbers. Moreover the conformational defects of the hexyl chains present a weak and structured absorption in the range 1375−1200 cm^{-1}.

(4) The existence of conformationally ordered or disordered hexyl chains is also indicated by the presence or absence of a fine structure in the >CH_2 symmetric stretching modes near 2850 cm^{-1} (D band).

(5) The intermolecular order of the −CH_3 groups, hence of the hexyl chains, is revealed by the occurrence of the splitting of the antisymmetric −CH_3 stretching band near 3000 cm^{-1} (A band).

6) The frequency of the =C−H out-of-plane mode is an unambiguous marker of both the shape of the thiophene backbone and of the conformational order of the hexyl chains: phase 1 strong and broad band near 820 cm^{-1}; phase 2 sharp and strong line peaked at 826 cm^{-1}; phase 3 (disordered) strong and broad band absorption at 840−830 cm^{-1}.

We are confident that the markers identified so far may be useful also for the molecular characterization of other regio-specific oligo or poly(3-alkylthiophene)s. Different length of the alkyl residues or different crystal forms may induce slight changes in the molecular vibrational dynamics, which we believe can be monitored by the spectroscopic tools presented here.

AUTHOR INFORMATION

Corresponding Authors

*(L.B.) E-mail: luigi.brambilla@polimi.it.

*(G.Z.) E-mail: giuseppe.zerbi@polimi.it.

Author Contributions

The manuscript was written through contributions of all authors. All authors have given approval to the final version of the manuscript.

Notes

The authors declare no competing financial interest.

ACKNOWLEDGMENTS

Authors thank Felix P. V. Koch and Paul Smith for providing the oligothiophenes and Günter Reiter for discussions. We acknowledge Chiara Castiglioni for her enthousiastic support all over the years. N.S. acknowledges her support by a European Research Council (ERC) Starting Independent Researcher Fellowship under Grant Agreement No. 279587 and a KAUST Competitive Research Grant (CRG-1-2012-THO-015).

REFERENCES

(1) Bäuerle, P. Sulfur-containing Oligomers, In *Electronic Materials: The Oligomer Approach*; Müllen, K., Wegner, G., Eds.; Wiley-VCH: Weinheim, Germany, 1998; pp105−197.

(2) Harrison, M. G.; Friend, R. H. Optical Applications In *Electronic Materials: The Oligomer Approach*; Müllen, K., Wegner, G., Eds.; Wiley-VCH: Weinheim, Germany, 1998; pp 515−558.

(3) Xin, H.; Kim, F. S.; Jenekhe, S. A. *J. Am. Chem. Soc.* **2008**, *130*, 5424−5425.

(4) Xin, H.; Ren, G.; Kim, F. S.; Jenekhe, S. A. *Chem. Mater.* **2008**, *20*, 6199−6207.

(5) Padinger, F.; Rittberger, R. S.; Sariciftci, N. S. *Chem. Rev.* **2007**, *107*, 1324−1338.

(6) *Handbook of Thiophene Based Materials: Applications in Organic Electronics and Photonics*; Perepichka, J. F., Perepichka, D. F., Eds.; John Wiley & Sons Ltd.: Chichester, U.K., 2009; Vol 2.

(7) Bolognesi, A.; Porzio, W.; Provasoli, F.; Ezquerra, T. *Macromol. Chem.* **1993**, *194*, 817−827.

(8) Bolognesi, A.; Porzio, W.; Provasoli, A.; Comotti, A.; Sozzani, P.; Simonutti, R. *Macromol. Chem. Phys.* **2001**, *202*, 2586−2591.

(9) Buono, A.; Sun, N. H.; Raos, G.; Gila, L.; Cominetti, A.; Catellani, M.; Meille, S. V. *Macromolecules* **2010**, *43*, 6772−6781.

(10) Dag, S.; Wang, L. W. *J. Phys. Chem. B* **2010**, *114*, 5997−6000.

(11) Baggioli, A.; Meille, S. V.; Raos, G.; Po, R.; Brinkmann, M.; Famulari, A. *Int. J. Quantum Chem.* **2013**, *113*, 2154−2162 and references herein..

(12) Mena-Osteriz, E.; Meyer, A.; Langeveld-Voss, B. M. W.; Janssen, R. A. J.; Meijer, E. W.; Bauerle, P. *Angew. Chem.* **2000**, *112*, 2792−2796.

(13) Zerbi, G.; Gussoni, M.; Castiglioni, C. Vibrational Spectroscopy of Policonjugated Aromatic Materials with Electrical Nonlinear Optical Properties In *Conjugated Polymers*; Brédas, J. L., Silbey, R., Eds.; Kluver: Amsterdam, 1991; pp 435−507;. Gussoni, M.; Castiglioni, C.; Zerbi, G. Vibrational Spectroscopy of Polyconjugated Materials: Polyacetylene and Polyenes. In *Spectroscopy of Advanced Materials*; Clark, R. J., Hester, P. E., Eds.; Wiley: New York, 1991; pp 261−353.

(14) Del Zoppo, M. E.; Castiglioni, C.; Zuliani, P.; Zerbi, G. Molecular and Electronic Structure and Nonlinear Optics of Polyconjugated Materials from Their Vibrational Spectra, In *Hanbook of Conducting Polymers*, 2nd ed.; Skotheim, T., Elsenbaumer, R. L., Reynolds, J. R., Eds.; Dekker: New York, 1998; Vol. 2, pp 765−882.

(15) Zerbi, G. Vibrational Spectroscopy of Conducting Polymers, Theory and Perspective. In *Vibrational Spectroscopy of Polymer*; Everall, N. J., Chalmers, J. M., Griffith, P. R., Eds.; Wiley: Chichester, U.K., 2007; pp 487−536.

(16) For applications in the development of new devices see, for instance: Tsoi, W. C.; James, D. T.; Kim, J. S.; Nicholson, P. G.; Murphy, C. E.; Bradley, D. D. C.; Nelson, J.; Kim, J. *J. Am. Chem. Soc.* **2011**, *133*, 9834−9843.

(17) Jianming Zhang, Y. Y.; Jian Hu, J. S.; Zhang, T.; Duan, Y. *Macromolecules* **2011**, *44*, 9341−9350.

(18) Jianming Zhang, Y. Y.; Sun, J. *Macromolecules* **2011**, *44*, 6128−6235.

(19) Yazawa, K.; Yamamoto, T.; Asakawa, N. *Phys. Rev. B* **2006**, *74*, 094204−1−094204−12.

(20) Rahimi, K.; Botiz, I.; Stingelin, N.; Kayunkid, N.; Sommer, M.; Koch, F. P. V.; Nguyen, H.; Coulembier, O.; Dubois, P.; Brinkmann, M.; Reiter, G. *Angew. Chem., Int. Ed.* **2012**, *51*, 11131−11135.

(21) Rahimi, K.; Botiz, I.; Agumba, J. O.; Motamen, S.; Stingelin, N.; Reiter, G. *RSC Adv.* **2014**, *4*, 11121−11123.

(22) Hourani, W.; Rahimi, K.; Botiz, I.; Koch, F. P. V.; Reiter, G.; Lienerth, P.; Heiser, T.; Bubendoff, J. L.; Simon, L. *Nanoscale* **2014**, *6*, 4774−4780.

(23) Lopez Navarrete, J. T.; Zerbi, G. *J. Chem. Phys.* **1991**, *94*, 957−964. Lopez Navarrete, J. T.; Zerbi, G. *J. Chem. Phys.* **1991**, *94*, 965−970.

(24) Zerbi, G.; Chierichetti, B.; Inganaas, O. *J. Chem. Phys.* **1991**, *94*, 4637−4645. Zerbi, G.; Chierichetti, B.; Inganaas, O. *J. Chem. Phys.* **1991**, *94*, 4646−4658.

(25) Zerbi, G.; Radaelli, R.; Veronelli, M.; Brenna, E.; Zotti, G. *J. Chem. Phys.* **1993**, *98*, 4531−4542.

(26) Koch, F. P. V.; Smith, P.; Heeney, M. *J. Am. Chem. Soc.* **2013**, *135*, 13695−13698.

(27) Frisch, M. J.; et al. *Gaussian 09*, Revision D.01; Gaussian Inc.: Wallingford CT, 2009.
(28) Merrick, J. P.; Moran, D.; Radom, L. *J. Phys. Chem. A* **2007**, *111* (45), 11683−11700.
(29) Prosa, T. J.; Winokur, M. J.; McCullough, R. D. *Macromolecules* **1996**, *29*, 3654.
(30) Natta, G.; Mazzanti, G.; Corradini, P. *Atti Acad. Naz. Lincei Cl. Sci. Fis. Mater. Nat. Rend.* **1958**, *25*, 3−7.
(31) Shirakawa, H.; Louis, E. J.; McDiarmid, A. G.; Chiang, C. K.; Heeger, A. *J. Chem. Soc. Chem. Commun.* **1977**, 578−580.
(32) Zerbi, G.; Castiglioni, C.; Gussoni, M. *Synth. Met.* **1991**, *41*, 3407−3412. Castiglioni, C.; Lopez-Navarrete, J. T. L.; Zerbi, G.; Gussoni, M. *Solid State Commun.* **1988**, *65*, 625−630. Castiglioni, C.; Tommasini, M.; Zerbi, G. *Phys. Trans. R. Soc. London A* **2004**, *362*, 2425−2459. Bianco, A.; Del Zoppo, M.; Zerbi, G. *J. Chem. Phys.* **2004**, *120*, 1450.
(33) Zerbi, G. Vibrational Spectra as a Probe of Structural Order/disorder in Chain Molecules and Polymers In *Modern Polymer Spectroscopy*; Zerbi, G., Ed.; Wiley-VCH: New York, 1999; pp 87−206.
(34) Su, W. P.; Schrieffer, J. R.; Heeger, A. *J. Phys. Rev. B* **1980**, *22*, 2099−2111. Su, W. P.; Schrieffer, J. R.; Heeger. *Phys. Rev. Lett.* **1979**, *42*, 1698−1701. Lu, Y. *Solitons and Polarons in Conducting Polymers*; World Scientific: Singapore, 1988.
(35) Ehrenfreund, E.; Vardeny, Z.; Brafman, O.; Horovitz, B. *Phys. Rev. B* **1987**, *36*, 1535−1553.
(36) Heeger, A. J. In *Hanbook of Conducting Polymers*, 2nd ed; Skotheim, T., Elsenbaumer, R. L., Reynolds, J. R., Eds.; Dekker: New York, 1998; Vol. *2*, pp 27−84.
(37) Bässler, H. Electronic Excitation In *Electronic Materials: The Oligomer Approach*; Müllen, K., Wegner, G., Eds.; Wiley-VCH: Weinheim, Germany, 1998; pp 403−431.
(38) Roth, S. *One Dimensional Metals*; VCH: Weinheim, Germany, 1995.
(39) Bubeck, C. Nonlinear Optical Properties of Oligomers, In *Electronic Materials: The Oligomer Approach*; Müllen, K., Wegner, G., Eds.; Wiley-VCH: Weinheim, Germany, 1998; pp 449−478.
(40) Rumi, M. C.; Zerbi, G.; Müllen, K.; Rehan, M. *J. Chem. Phys.* **1997**, *106*, 24−34.
(41) Chandrasekhar, P. In *Conducting Polymers: Fundamentals and Applications*; Kluver: Boston, MA, 1999.
(42) Rimai, L.; Heyde, M. E.; Gill, D. *J. Am. Chem. Soc.* **1973**, *95* (14), 4493−4501.
(43) Jones, R. N.; Sandorfy, C. Application of Infrared and Raman Spectrometry to the Elucidation of Molecular Structure in *Chemical Applications of Spectroscopy. Technique of Organic Chemistry*; Weissenberger, A., Ed.; Interscience: New York, 1956; Vol. *9*, pp 247−580.
(44) Socrates, G. *Infrared Characteristic Group Frequencies*, 2nd ed.; Wiley: New York, 1980.
(45) Zerbi, G.; Ciampelli, F.; Zamboni, V. *J. Polym. Sci. C* **1964**, *7*, 141−151.
(46) Zerbi, G. Vibrational Spectra as a Probe of Structural Order/disorder in Chain Molecules and Polymers In *Modern Polymer Spectroscopy*; Zerbi, G. ed.; Wiley-VCH: New York, 1999; p 113.
(47) Gussoni, M.; Castiglioni, C.; Zerbi, G. *J. Phys. Chem.* **1984**, *88*, 600−604.
(48) Henry, B. R.; Siebrand, W. *J. Chem. Phys.* **1968**, *49*, 5369−5376.
(49) McKean, D. C. *Chem. Soc. Rev.* **1978**, *7*, 399−422.
(50) Zerbi, G.; Castiglioni, C.; Del Zoppo, M. Structure and Optical Properties of Conjugated Oligomers from Their Vibrational Spectra In *Electronic Materials: The Oligomer Approach*; Müllen, K., Wegner, G., Eds.; Wiley-VCH: Weinheim, Germany, 1998; pp 345−402.
(51) Rico, M.; Orza, J. M.; Morcillo. *J. Spectrochim. Acta B* **1965**, *21*, 689−719.
(52) Schachtschneider, J. H.; Snyder, R. G. *Spectrochim. Acta* **1965**, *21*, 1527−1542.
(53) Maroncelli, M.; Snyder, R. G.; Qi, P.; Strauss, H. L.; Snyder, R. G. *J. Am. Chem. Soc.* **1982**, *104*, 6237−6247.
(54) Jona, P.; Gussoni, M.; Zerbi, G. *J. Appl. Phys.* **1985**, *57*, 834−841.
(55) Castiglioni, C.; Gussoni, M.; Zerbi, G. *J. Chem. Phys.* **1991**, *95*, 7144−7149.
(56) Gaber, B. P.; Peticolas, W. *Biochim. Biophys. Acta* **1977**, *465*, 260−274.
(57) Levin, I. W. Vibrational Spectroscopy of Membrane Assemblies In *Advances in Infrared and Raman Spectroscopy*; Clark, R. J. H., Hester, R. E., Eds.; Wiley-Heyden: New York, 1983; Vol. *11*, pp 1−48.
(58) Flory, P. J. *Statistical mechanics of chain molecules*; Wiley Interscience: New York, 1969.
(59) Zerbi, G.; Magni, R.; Gussoni, M.; Holland-Moritz, K.; Bigotto, A.; Dirlikov, S. *J. Chem. Phys.* **1981**, *75*, 3175−3194 and references herein..
(60) Mansfield, M. L.; Boyd, R. H. *J. Polym. Sci., Polym. Phys. Ed.* **1978**, *16*, 1227−1252.
(61) Mansfield, M. L. *Chem. Phys. Lett.* **1980**, *69*, 383−385.
(62) Skinner, J. L.; Wolines, P. J. *J. Chem. Phys.* **1980**, *73*, 4015−4021.
(63) Klein, M. L. *J. Chem. Soc. Faraday Trans.* **1992**, *13*, 1701−1705.
(64) Wilson, E. B.; Decius, J. C.; Cross, P. C. *Molecular Vibrations*; McGraw-Hill: New York, 1955; p 364.
(65) Zerbi, G.; Del Zoppo, M. *J. Chem. Soc. Faraday Trans.* **1992**, *88*, 1835−1844.
(66) Zerbi, G.; Piazza, R.; Holland-Moritz, K. *Polymer* **1982**, *23*, 1921−1928.
(67) Askadskaya, L.; Rabe, J. P. *Phys. Rev. Lett.* **1992**, *69*, 1395−1398.
(68) Jona, P.; Bassetti, B.; Benza, V.; Zerbi, G. *J. Chem. Phys.* **1987**, *86*, 1561−1566.
(69) The peak frequencies in the spectral pattern observed in the CH stretching range show changes which are necessarily associated with the environment around the alkyl chains. Gaber and Peticolas[56] as well as Levin at al.[57] reported that when a fully crystallized long alkyl chain melts the peaks of the $>CH_2$ stretchings broaden and shift toward higher frequencies. This observation was taken for a long time as evidence of alkyl "chain melting" or "chain disordering" or "lateral melting". Originally chain melting was described as the collapse of the chain in a conformationally disordered structure with a temperature dependent distribution of conformers (e.g., GTG′, GTG, TGGT, etc.) possibly ruled by Flory's rotational isomeric state model.[58] Later the concept of "lateral disorder" has been developed for *n*-alkanes, which show the existence of an intermediate phase (α phase, or rotatory phase) a few degrees below melting.[59] It was realized that, if the physical space around chains is favorable, chains can keep an average straight shape and can perform librations around their axes. Molecules can librate as a rigid rod with hindered large amplitude rotational motions or because of thermally driven small amplitude conformational distortions which, in some cases, can propagate along the chain.[60−63] In any case, the classical simple dynamical treatment of molecular vibrations by Wilson shows that, within the $-CH_2-CH_2-$ group, there is a kinetic energy coupling between CH stretching and the torsional angle about the C−C bond. Hence a shift of the CH stretching must occur when the conformation of the C−C−C−C angle changes substantially.[64]